

# Tool condition monitoring based on numerous signal features

Krzysztof Jemielniak · Tomasz Urbański ·  
Joanna Kossakowska · Sebastian Bombiński

Received: 31 March 2011 / Accepted: 26 June 2011 / Published online: 22 July 2011  
© The Author(s) 2011. This article is published with open access at Springerlink.com

**Abstract** This paper presents a tool wear monitoring strategy based on a large number of signal features in the rough turning of Inconel 625. Signal features (SFs) were extracted from time domain signals as well as from frequency domain transforms and their wavelet coefficients (time–frequency domain). All of them were automatically evaluated regarding their relevancy for tool wear monitoring based on a determination coefficient between the feature and its low-pass-filtered course as well as the repeatability. The selected SFs were used for tool wear estimation. The accuracy of this estimation was then used to evaluate the sensor and signal usability.

**Keywords** Tool condition monitoring · Signal feature selection · Aerospace material

## Abbreviations

SF	Signal feature
TCM	Tool condition monitoring
AE	Acoustic emission
RMSE	Root mean square error

## 1 Introduction

The search for process automation, stimulated by growing demands for higher quality and productivity, and a reduction in the human supervision of a machining process,

has resulted in the development of tool condition monitoring (TCM) systems. It is generally acknowledged that reliable process condition monitoring based on a single signal feature (SF) is not feasible [1]. The development of a robust and reliable tool condition monitoring system requires the application of the most meaningful SFs which best describe the tool wear [1–4]. Therefore, the key issue in a TCM system is calculating a sufficient number of SFs related to tool and/or process conditions [1, 4–6]. Various methods for tool wear monitoring have been developed, most often based on cutting forces, acoustic emission (AE), and vibrations [2, 6, 7]. The sensor signal has to be transformed into features that could describe the signal adequately while simultaneously maintaining the relevant information about tool conditions in the extracted features. There are several SFs that can be extracted from any time domain signal, including the average, effective value, variance, skewness, kurtosis, etc. [1, 5, 6]. Sometimes, a signal is transformed into a frequency or time–frequency domain (fast Fourier transform, wavelet transform, etc.), and then the signal features are extracted from these transforms. There can be many different descriptors from different sensor signals, most of which are hardly related to the monitoring process. Therefore, a feature selection procedure is necessary. Relevant features are then used for tool or process condition diagnosis.

The information extracted from one or several sensors' signals has to be combined into one tool condition estimation. This can be achieved by various means such as statistical methods, autoregressive modeling, pattern recognition, expert systems, and others [1, 5, 6]. The neural network approach has recently been the most intensively studied method for feature fusion [5]. Usually, a single neural network is used, where several SFs are fed into the network inputs while the tool wear estimation is the

K. Jemielniak (✉) · T. Urbański · J. Kossakowska · S. Bombiński  
Faculty of Production Engineering,  
Warsaw University of Technology,  
Narbutta 86,  
02-534 Warsaw, Poland  
e-mail: k.jemielniak@wip.pw.edu.pl

network output. An alternative approach is the use of a hierarchical tool wear monitoring algorithm [4].

Tool wear is an especially severe problem when machining nickel-based heat-resistant super alloys such as Inconel 625, which are employed in aeronautic and aerospace applications because of their high shear strength, work hardening tendency, highly abrasive carbide particles, tendency to weld and form a built-up edge, and low thermal conductivity [8]. All of these difficulties lead to high tool wear and compromise the attainment of high material removal rates. While machining Inconel 625, the cutting tool often bears extreme thermal and mechanical loads close to the cutting edge, leading to rapid tool wear. Therefore, tool wear is not repeatable and has a tendency to finish catastrophically (chipping or breakage of the cutting edge). Tool condition monitoring under such conditions seems to be especially important. The objective of this paper was to compare the usability of various signals and signal features originating from three sensors—cutting force, vibration, and acoustic emission—which are used to monitor the tool condition during the rough machining of Inconel 625. New algorithms for signal feature selection and elimination and training of the system were applied based on data acquired in subsequent tool lives.

## 2 Experimental setup and conditions

The workpieces were impeller cases made of Inconel 625 (Fig. 1a) and machined with subsequent perpendicular cuts from a 406- to 268-mm diameter, with the depth of the cut,  $a_p=2.5$  mm; feed,  $f=0.2$  mm/rev; and cutting speed,  $v_c=220$  m/min. The tool was a CRSNL with whisker-reinforced round ceramic inserts, RNGN CC670 (Fig. 1a). The tool life was limited by three phenomena: tool notch wear (Fig. 1b), burr formation (Fig. 1c), and a drastic decrease in the surface finish. Notch wear appeared in the region where

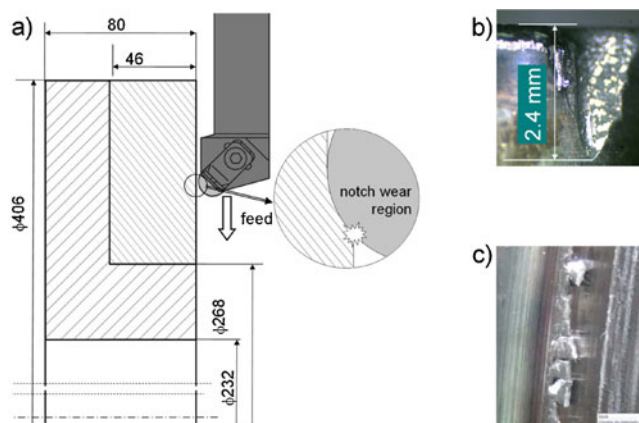


**Fig. 1** Workpiece and tool (a) and tool life criteria: tool wear (b), burrs (c), surface roughness (d)

the machined surface, hardened by previous cut, contacted the cutting edge (see Fig. 1a). Sometimes, despite the high value of this wear, the cutting edge region shaping the workpiece surface was still intact and the surface finish was still acceptable. The notch wear was often accompanied by burr formation (Fig. 1c), but this was not always the case. Thus, all three phenomena appeared autonomously, making the determination of the tool life end difficult, subjective, and dependant on the machine tool operator's experience. Here, the used-up portion of the tool life ( $\Delta T$ ), defined as the ratio of the cutting time as performed so far ( $t$ ) to the overall tool life span ( $T$ ), was used as the tool condition measure. Three workpieces were machined, during which seven tools were worn out. A higher number of used tools (tool lives) than machined workpieces is characteristic when machining large aerospace parts. Therefore, the application of a TCM system is especially desirable.

The experiments were performed on a turning center (TKX 50N) equipped with an industrial AE sensor (Kistler 8152B121) and accelerometer (PCB PIEZOTRONICS 356A16) mounted on the turret and a cutting force sensor (Kistler 9017B) mounted under the turret. A raw AE ( $AE_{raw}$ ) signal was acquired with a sampling frequency of 2 MHz using a DAQ card, NI PCI 6111. As this sampling frequency produces an enormously large amount of data, only 0.05 s (100,000 samples) out of every 10-s period was recorded and analyzed. The demodulated amplitude of the AE signal ( $AE_{RMS}$ ), two cutting force signals ( $F_x$  and  $F_z$ ), and two vibration signals ( $V_y$  and  $V_z$ ) were acquired simultaneously with a sampling frequency of 30 kHz using an NI PCI 6221 DAQ card at the same points of time (every 10 s) during 1.66 s (50,000 samples each). Each cut lasted 96 s, during which time eight such recordings of the signals were taken and treated as separate, subsequent measurements, used for tool wear monitoring.

## 3 Signal processing

### 3.1 Signal feature extraction

As it is really not possible to predict which SFs will be useful in a particular case, as many as possible should be extracted from the available signals. Then, those that are informative, correlated with tool wear, should be selected for tool condition monitoring. Here, from each of six signals ( $F_x$ ,  $F_z$ ,  $V_y$ ,  $V_z$ ,  $AE_{raw}$ , and  $AE_{RMS}$ ), five time domain signal features were extracted:

- Effective value (e.g.,  $F_{x,RMS}$ ),
- Standard deviation (e.g.,  $F_{x,StDev}$ ),
- Skewness (e.g.,  $F_{x,Skew}$ ),

- Kurtosis (e.g.,  $F_{x,Kurt}$ ), and
- Crest factor (the ratio of the peak level to the rms level, e.g.,  $F_{x,Crest}$ ).

Fast Fourier transform was applied to obtain eight frequency domain features from each signal:

- Dominant frequency, e.g.,  $F_{x,DF}$ ,
- Power in dominant band, e.g.,  $F_{x,PDB}$ ,
- Power in band 62–125 Hz, e.g.,  $F_{x,P62-125}$ ,
- Power in band 125–250 Hz, e.g.,  $F_{x,P125-250}$ ,
- Power in band 250–500 Hz, e.g.,  $F_{x,P250-500}$ ,
- Power in band 500–1,000 Hz, e.g.,  $F_{x,P500-1000}$ ,
- Power in band 1,000–2,000 Hz, e.g.,  $F_{x,P1000-2000}$ , and
- Power in band 2,000–4,000 Hz, e.g.,  $F_{x,P2000-4000}$ .

A three-level wavelet packet transform (WPT) decomposition was used to obtain 14 coefficients, called approximations  $A$  and details  $D$ , which are band pass signals (see Fig. 2). From each of these coefficients, six time–frequency domain features were calculated:

- Logarithmic energy (e.g.,  $F_{x,ADA,E}$  is the energy of wavelet coefficient ADA of signal  $F_x$ ),
- Skewness (e.g.,  $F_{x,ADA,Skew}$ ),
- Kurtosis (e.g.,  $F_{x,ADA,Kurt}$ ),
- Effective value (e.g.,  $F_{x,ADA,RMS}$ ),
- Threshold crossing rate (number of times the signal crosses the threshold level, e.g.,  $F_{x,ADA,Count}$ ), and
- Pulse width (the percentage of time during which the signal remains above this threshold, e.g.,  $F_{x,ADA,Pulse}$ ).

Thus, there were 84 wavelet-based SFs calculated from each signal. Altogether, there were 582 signal features calculated automatically (97 from each of the six available signals, 194 SFs from each sensor).

### 3.2 Signal feature selection

While the number of extracted signal features is very large, some of them are very distorted, hardly dependent on tool

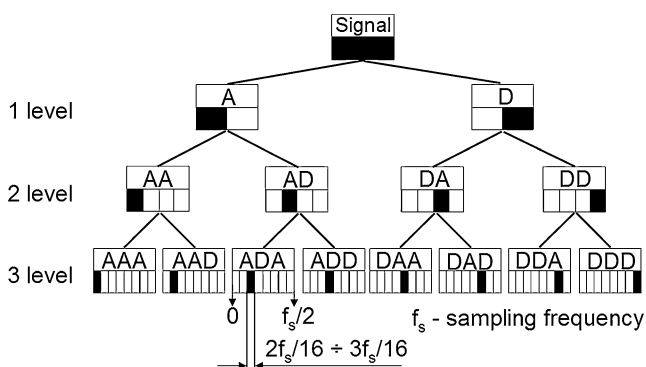


**Fig. 2** Three-level WPT decomposition; *blackened fields* indicate the frequency band of original signal

wear (e.g., Fig. 3a), while others are dependant mainly on the tool position on the workpiece (e.g., Fig. 3b). There are, however, SFs that are dependent on the tool condition (e.g., Fig. 3c), even if some also depend on the tool position (e.g., Fig. 3d). Only those SFs that are relevant and sensitive to tool conditions should be selected [5].

To measure this relevancy, a model for the relationship between the SF and tool wear or used-up-part-of-tool-life  $\Delta T$  is necessary. Here, a low-pass-filtered signal feature was accepted as an SF( $\Delta T$ ) model, which made it possible to avoid any uncertain suppositions about the mathematical formula of this model. Because the filter characteristic depends on the number of elements in a filtered time series, a SF is first normalized in time to 0–100% of the tool life ( $SF_T$ ), then  $SF_T$  is filtered to  $SF_{Tf}$  using a second-order Butterworth filter and a low cutoff frequency of 2% of the sampling frequency. Signal feature usability for tool condition monitoring can be evaluated using the coefficient of determination,  $R_s^2$ , which is a statistical measure of how well the  $SF_{Tf}(\Delta T)$  model approximates the real  $SF_T(\Delta T)$  relationship, or, in other words, how much this model is better than just the average value of  $SF_T$ .

$$R_s^2 = \frac{\sum_i (SF_{Ti} - SF_{Tav})^2 - \sum_i (SF_{Ti} - SF_{Tfi})^2}{\sum_i (SF_{Ti} - SF_{Tav})^2} \quad (1)$$

where  $\sum_i (SF_{Ti} - SF_{Tav})^2$  is the total square sum and  $\sum_i (SF_{Ti} - SF_{Tfi})^2$  is the residual square sum.

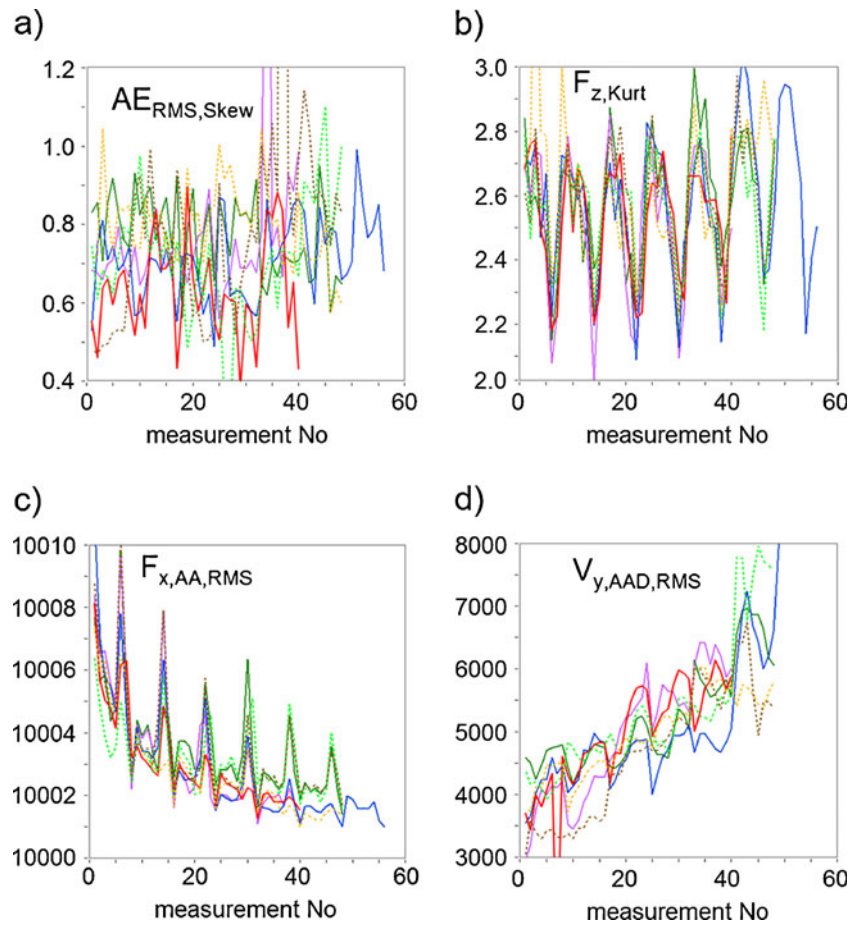
$SF_{Ti}$  and  $SF_{Tfi}$  are the single values of  $SF_T$  and  $SF_{Tf}$  respectively ( $i=0\dots100$ ), and  $SF_{Tav}$  is the average value of  $SF_T$ .

Because the TCM system should be able to monitor the tool wear already after the first tool life, this evaluation is based on the signals acquired during this first tool life. These SFs, for which  $R_s^2 > 0.4$ , are assumed to be satisfactorily correlated with the tool condition and, thus, useful. Figure 4 presents examples of SFs that are qualified and rejected by this criterion.

On the other hand, the selected SFs should not be strongly correlated to each other to avoid multiplication of the same information. Therefore, the SFs that meet the criterion are then sorted into a descending order, according to the  $R_s^2$  values. Then, the first (best) is selected and the correlation coefficients ( $r^2$ ) between this SF and every other SF are calculated. SFs with  $r^2 > 0.8$  are rejected as these too correlated with the best one. From among the remaining signal features, again, the best one is selected, and the SFs correlated with it are rejected. The procedure is repeated until no SF meeting the  $R_s^2 > 0.4$  criterion remains. Here, out of all 582 signal features, 133 SFs were automatically selected as useful, but after the elimination of similar SFs, only 40 remained.

After completion of the second tool life, the tool feature selection is repeated using all of the available data. Thus,

**Fig. 3** Examples of signal features calculated from available signals during all seven tool lives: skew of  $AE_{raw}$  signal (a), kurtosis of  $F_z$  signal (b), energy of WPT coefficient ADD of  $V_y$  signal (c), and standard deviation of  $F_x$  signal (d)



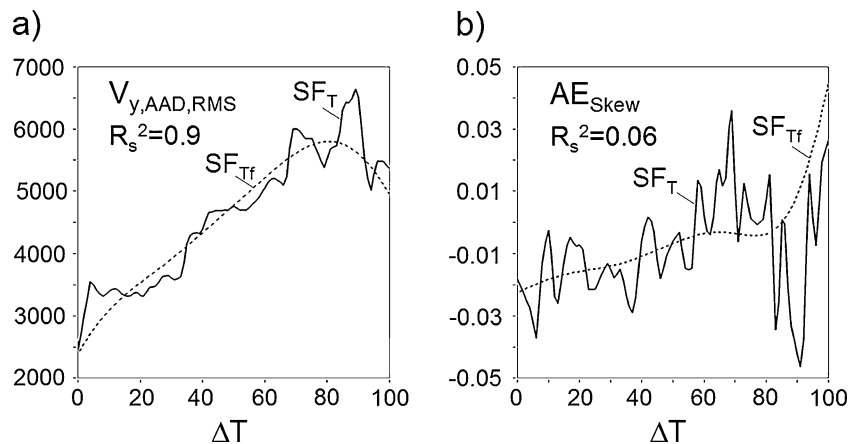
$R_s^2$  coefficients are calculated for both tool lives and averaged. Now, the application of the second, even more important, SF usability criterion can be applied: repeatability. It is evaluated using another determination coefficient,  $R_r^2$ :

$$R_r^2 = \frac{\sum_j \sum_i (SF_{Tfji} - SF_{2Tfav})^2 - \sum_j \sum_i (SF_{Tfji} - SF_{Tfavi})^2}{\sum_j \sum_i (SF_{Tfji} - SF_{2Tfav})^2} \quad (2)$$

where  $SF_{Tfji}$  is the value of  $SF_{Tf}$  in the  $i$ th point ( $i=0 \dots 100$ ) and  $j$ th tool life ( $j=1 \dots 2$ ),  $SF_{Tfavi} = \frac{1}{2} \sum_j SF_{Tfji}$  is the average of  $SF_{Tf}$  in  $i$ th point, and  $SF_{2Tfav} = \frac{1}{202} \sum_j \sum_i SF_{Tfji}$  is the average of all  $SF_{Tf}$  values in two tool lives.

These SFs for which  $R_r^2 > 0.6$  are assumed to be sufficiently repeatable. All of the SFs that meet both criteria are sorted according to their  $R_r^2$  values. The elimination of the SFs that are correlated to each other is based on the data

**Fig. 4** Examples of SFs that met the  $R_s^2 > 0.4$  criterion (a) and those rejected by this criterion (b)



for two tool lives. One hundred eight SFs were recognized as useful and repeatable, but after the elimination of similar SFs, only 39 remained.

After the end of the third tool life, the entire SF selection and elimination procedure is again repeated using all of the available data. Figure 5 presents examples of the signal features accepted by both criteria and recognized as correlated with the tool wear, but not repeatable and thus rejected. Finally, there were 62 relevant and repeatable signal features, out of which 27 appeared to be not similar to each other. The signal features selected in this way were used for tool wear monitoring in all of the subsequent tool lives, beginning from the fourth one.

It must be stressed that the signal features that qualified after the first tool life did not have to be selected after two or three tool lives, e.g., the SFs selected from the accelerometer sorted according to  $R_s^2$  after the first tool life and accordingly to  $R_r^2$  after the second and third tool lives were:

- After the first tool life:  $V_{z,ADA,E}$ ,  $V_{y,RMS}$ ,  $V_{y,Crest}$ ,  $V_{z,D,Skews}$ ,  $V_{z,DDA,Kurt}$ ,  $V_{z,AD,Pulse}$ ,  $V_{y,P250-500}$ ,  $V_{z,AAD,Kurt}$ ,  $V_{z,Kurt}$ ,  $V_{y,A,RMS}$ ,  $V_{y,AD,Kurt}$ ,  $V_{z,AD,Kurt}$ ,  $V_{z,DAA,Kurt}$ ,  $V_{z,DDA,Count}$
- After two tool lives:  $V_{y,Crest}$ ,  $V_{z,StDev}$ ,  $V_{y,D,Pulse}$ ,  $V_{z,AAD,RMS}$ ,  $V_{y,P4000-8000}$ ,  $V_{y,AAD,Kurt}$ ,  $V_{y,DA,E}$ ,  $V_{y,AAA,Kurt}$ ,  $V_{y,AD,RMS}$ ,  $V_{y,A,RMS}$ ,  $V_{y,AD,Count}$ ,  $V_{z,P250-500}$ ,  $V_{z,P500-1000}$ ,  $V_{z,AAD,Kurt}$
- After three tool lives:  $V_{y,D,Pulse}$ ,  $V_{y,AAD,RMS}$ ,  $V_{y,P4000-8000}$ ,  $V_{y,AAA,Kurt}$ ,  $V_{z,StDev}$ ,  $V_{y,A,RMS}$

Figure 6 shows the numbers of SFs selected after the first tool life and the three tool lives for each sensor. The latter are also shown for each signal. As can be seen, the force sensor produced the highest number of useful, relevant SFs, meaning those that were well correlated with the tool condition, repeatable, and not similar to each other. The data presented in Fig. 6 show that the cutting force component,  $F_x$  (perpendicular to the cutting speed vector),

is a source of more potentially useful SFs than  $F_z$  (parallel to the cutting speed vector), and the vibration in the  $y$  direction is also more informative than that parallel to the cutting speed. The AE sensor produced the smallest number of useful signal features from both the low- and high-frequency signals ( $AE_{RMS}$  and  $AE_{raw}$ , respectively).

It may be interesting to consider the possibility of using the signals singly and in various combinations. Such a comparison is presented in Table 1 (SFs only after three tool lives). As can be seen, the number of useful signal features selected from two signals does not have to be the sum of the SF numbers selected from the signals separately because the SFs calculated from one sensor can be correlated to the SFs calculated from another signal.

Because the cutting force sensor is much more difficult to install than the vibration and AE sensors installed on the surface of the machine tool, it is worth considering using them without the cutting force sensor. Another option worth considering is dropping the  $AE_{raw}$  signal, which requires much more demanding signal processing and a separate DAQ device (high sampling frequency). In both cases, the number of useful SFs for tool condition monitoring appears to be the sum of the SFs obtained from separate signals.

#### 4 Decision-making algorithm

Tool wear estimation is based on a hierarchical algorithm [4]. In the first step of the algorithm, the used-up portion of the tool life ( $\Delta T$ ) is evaluated using every selected signal feature separately [9].

##### 4.1 Tool condition estimation based on single signal feature

Here, the tool condition is estimated on the basis of a signal feature, the used-up portion of tool live model in the form of function  $SF_{Tf}(\Delta T)$ , which is an array of 101 elements (0–100% of  $\Delta T$ ) –  $SF_{Tf}[\Delta T]$ .

**Fig. 5** Examples of the evaluation of signal features’ repeatability based on data from three tool lives: SF which met the criterion (a) and SF that was rejected as not repeatable despite being correlated with tool wear (b)

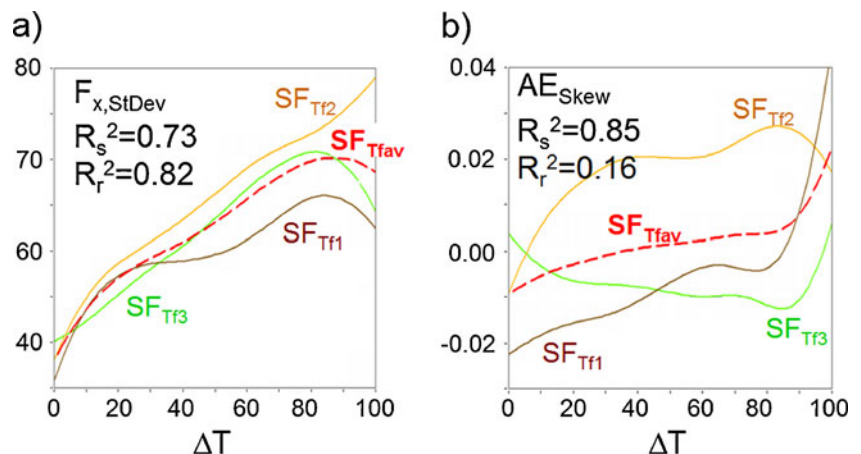
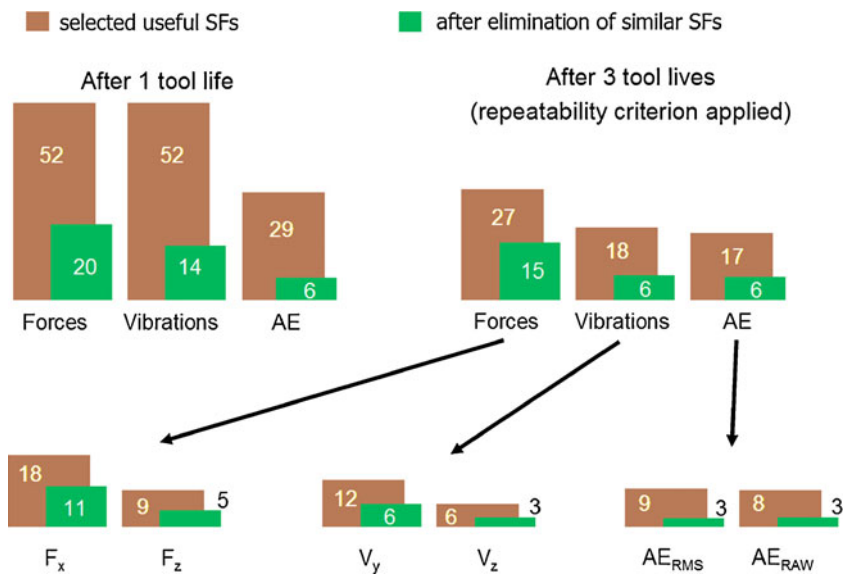


**Fig. 6** Number of useful SFs selected from each sensor signal before and after elimination of similar SFs



After subsequent signal measurements, the system calculates the signal feature value  $SF[n]$ , where  $n$  is the number of measurements (data acquisitions). Then, the  $SF_{Trf}[\Delta T]$  array created after the preceding tool lives is searched for the values closest to  $SF[n]$  (Fig. 7a). It may happen that after the next measurement, the SF value corresponds to a value of the used-up portion of the tool life lower than that reached in the previous operation (Fig. 7b). Such a system indication might be disorienting for the operator. Therefore, the search starts from the  $\Delta T$  value obtained after the previous measurement, which means that the used-up portion of the tool life presented to the operator cannot decrease. Sometimes it happens that the SF value is affected by some disturbance and corresponds to a very large increase in the tool wear. To remedy such a mistake, the search for the SF value is limited to 30 elements of the  $SF_{Trf}[\Delta T]$  array created after the preceding tool lives array, i.e., to 30% of the tool life (see Fig. 7c). This means that in the case of accelerated tool wear, the system allows three operations to be performed before it signals a tool failure. This procedure also has another purpose, namely, it enables signal features that are not monotonic with respect to the used-up portion of the tool life to be utilized, at least to

some extent, as presented in Fig. 7d. In the example shown here, the signal feature value corresponds to  $\Delta T=63\%$  and  $\Delta T=95\%$ . The restriction of the array search to 30% of  $\Delta T$  indicates that  $\Delta T=63\%$ .

#### 4.2 Integration of tool condition estimations

Separate tool condition estimations based on each useful signal feature are integrated in the next step of the algorithm (Fig. 8). All of the  $\Delta T$  estimations are averaged and displayed as the final tool condition evaluation. This value is used as the initial value,  $\Delta T_B$ , in the next iteration of the algorithm (after the next measurement).

The tool condition monitoring results obtained for each sensor used separately and for all of the sensors used together are presented in Fig. 9 as the used-up portions of tool lives evaluated by the system,  $\Delta T_{ev}$ , vs. the actual values of  $\Delta T$ . As the first tool life was used only for system training, the results of the six following tool lives are presented there. The second tool (dashed line with circles) was monitored using only data gathered during the first tool life, the third tool (dashed line with triangles) was monitored using data from the first two tool lives, while tools 4–7 (solid lines) were monitored using data from tool lives 1–3.

The accuracy of the tool condition monitoring evaluation can be assessed using the root mean square error (RMSE):

$$RMSE = \sqrt{\frac{1}{n} \sum_i (\Delta T_{ev} - \Delta T)^2} \tag{3}$$

The  $\Delta T$  values are expressed as percentages; thus, the RMSEs can be interpreted as average percentage errors. The RMSEs are also presented in Fig. 9.

As can be seen in Fig. 9a, the best results (RMSE=8.7) were obtained using the cutting force sensor, which is not

**Table 1** Numbers of SFs selected from various combination of signals after three tool lives – number of all SFs meeting criteria  $R_s^2 > 0.4$  and  $R_r^2 > 0.6$ /number of SFs after elimination of similar SFs

$F_x$	$F_z$	$V_y$	$V_z$	$AE_{RMS}$	$AE_{raw}$
18/11	9/5	16/6	6/3	9/3	8/3
21/15		18/6		17/6	
		27/9			
		35/12			
		62/27			

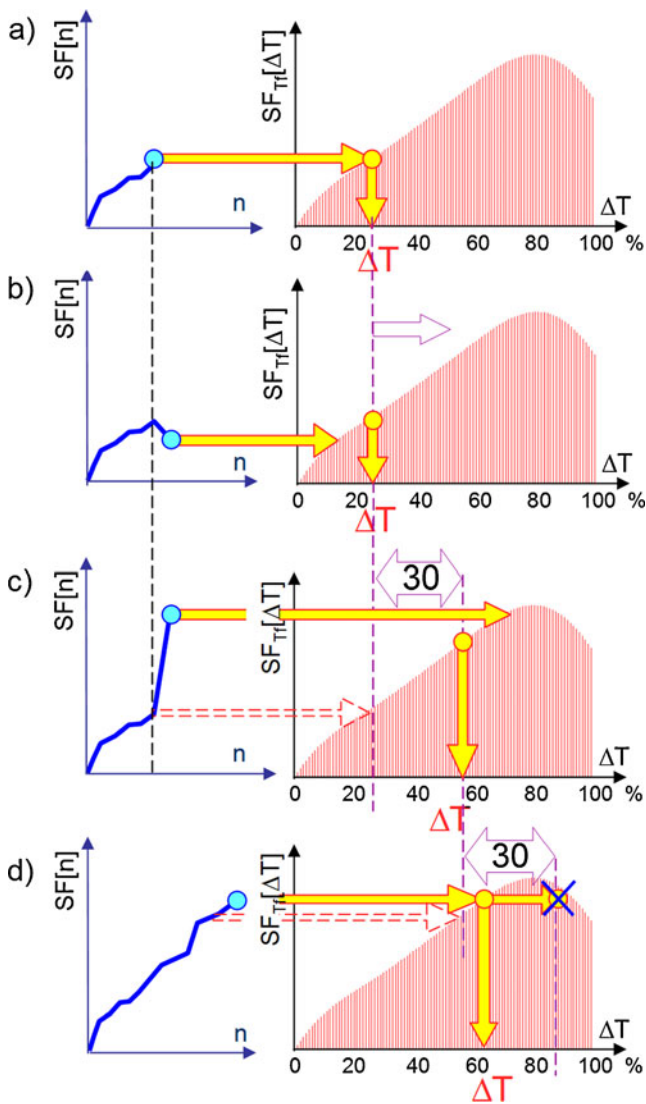


**Fig. 7** Used-up portion of tool life evaluation based on single signal feature. **a** Search of array  $SF_{Ti}[\Delta T]$  for the value closest to  $SF[n]$  obtained after the last signal measurement. **b** Search started from previous result; thus,  $\Delta T$  value cannot diminish. **c** Search limited to 30 elements of  $SF_{Ti}[\Delta T]$  array to reduce the influence of accidental high values. **d** Enabling the use of non-monotonic signal features

surprising—cutting force signals are commonly recognized as the most informative for tool condition monitoring. Here, this signal produced the highest number of useful signal features (see Fig. 6). The results achieved using the vibration sensor were also relatively good (Fig. 9b, RMSE=13.4), but much worse than those obtained using the force sensor, which could be expected from the lower number of useful signal features (Fig. 6). Not much worse were the results based on AE signals (Fig. 9c, RMSE=14.4), which produced a similar number of good SFs. All of the signals used together (Fig. 9d) produced results a little worse than the force sensor alone, which means that the poorly

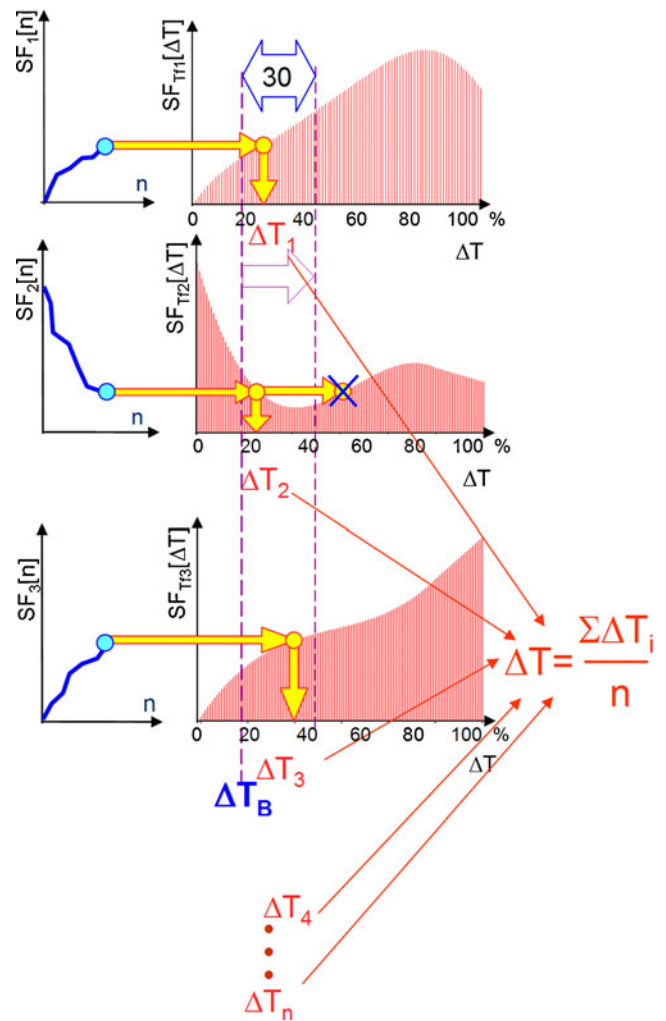
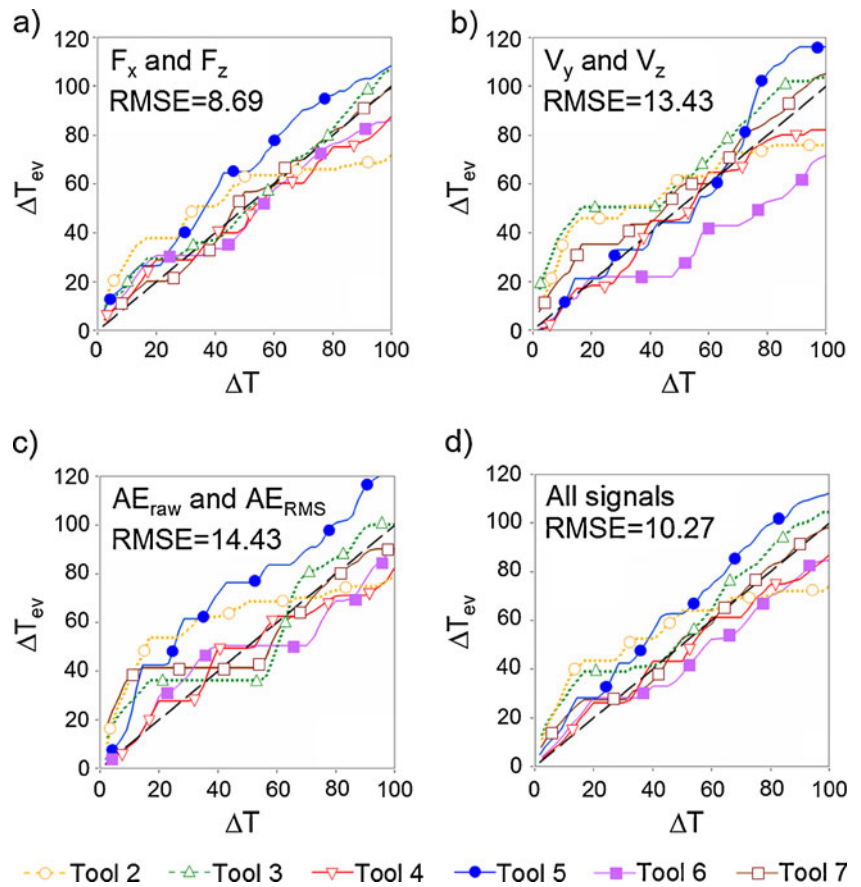


**Fig. 8** Hierarchical tool condition estimation

repeatable AE signal features had a negative influence on this result.

Again, it is worth considering the possibility of using single signals separately. Such a comparison is presented in Fig. 10. If the force sensor measured only one component ( $F_x$  or  $F_z$ ), the TCM system performance would be worse than for both available signals, which is caused by the useful SFs presented in Fig. 6. The  $F_x$  signal alone produced much better results than the  $F_z$  signal, which is a well-known phenomenon in tool condition monitoring. Vibration signals also allow for a better tool wear estimation when used together rather than separately, and the direction perpendicular to the cutting direction is more informative than that parallel to cutting. Finally, the AE sensor produced two signals in different frequency ranges (AE<sub>RMS</sub> and AE<sub>rms</sub>): When the signals were used separately, each achieved results that were half as good (higher RMSE) as the cutting force signals, which was the result of the very small number of useful SFs. This time,

**Fig. 9** Used-up portion of tool life evaluated by TCM system ( $\Delta T_{ev}$ ) vs. actual portion ( $\Delta T$ ) after training on selected signals



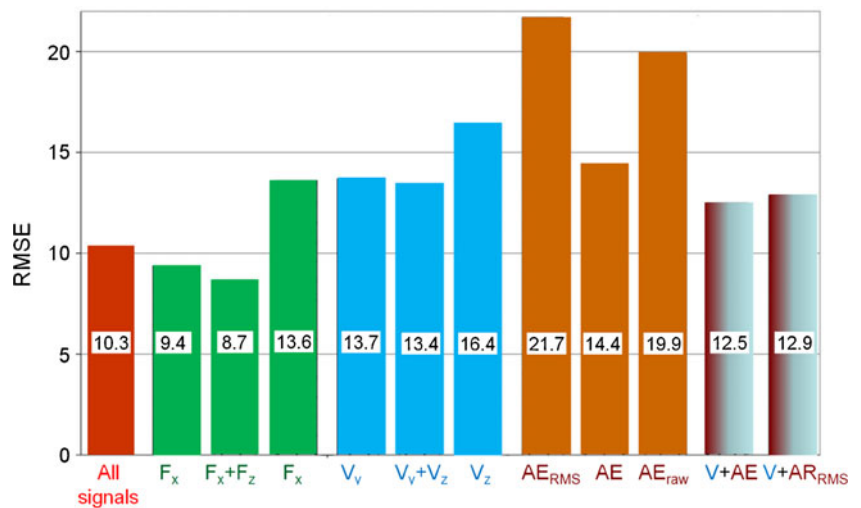
merging the two signals allows the highest improvement in the result, making it only a little worse than that achieved using vibration signals. The application of just the vibration and AE sensors, which are much easier to install than the cutting force sensor, results in an RMSE=12.5, which is better than that achieved by the sensors separately. The removal of the  $AE_{raw}$  signal, which requires a much higher sampling frequency, does not

result in substantial worsening of the RMSE error in this application.

**5 Conclusions**

Advanced signal processing methods offer a large number of possible signal features. It is impossible to predict in

**Fig. 10** Root mean square errors of tool wear monitoring based on various combinations of signals





advance which ones will be useful for tool condition monitoring in a particular application. Therefore, efficient methods to evaluate their usability have to be applied. The methodology proposed here was based on:

- Modeling the signal feature dependence on the used-up portion of tool life by low-pass filtering of the feature,
- Qualification of SF usability using a determination coefficient between the feature and its low-pass-filtered estimate and SF repeatability, and
- Elimination of similar (correlated with each other) signal features.

This methodology proved its effectiveness under very difficult cutting conditions where the number of tool lives is less than the number of the machined parts. A tool condition monitoring strategy based on a hierarchical algorithm was also tested, and the results achieved show that it is worth implementing on a factory floor in many applications.

**Acknowledgment** Financial support of Structural Funds in the Operational Program—Innovative Economy (IE OP) financed from the European Regional Development Fund—Project “Modern material technologies in aerospace industry”, no. POIG.0101.02-00-015/08 is gratefully acknowledged.

**Open Access** This article is distributed under the terms of the Creative Commons Attribution Noncommercial License which permits any noncommercial use, distribution, and reproduction in any medium, provided the original author(s) and source are credited.

## References

1. Teti R, Jemielniak K, O’Donnell G, Dornfeld D (2010) Advanced monitoring of machining operations. *CIRP Annals—Manuf Technol* 59:717–739
2. Cho S, Binsaeid S, Asfour S (2010) Design of multisensor fusion-based tool condition monitoring system in end milling. *Int J Adv Manuf Technol* 46:681–694
3. Li X (2002) A brief review: acoustic emission method for tool wear monitoring during turning. *Int J Mach Tools Manuf* 42:157–165
4. Jemielniak K, Bombiński S (2006) Hierarchical strategies in tool wear monitoring. *Proc IMechE J Eng Manuf* 220B:375–381
5. Abellan-Nebot JV, Subirón FR (2010) A review of machining monitoring systems based on artificial intelligence process models. *Int J Adv Manuf Technol* 47:237–257
6. Dimla DE (2000) Sensor signals for tool-wear monitoring in metal cutting operations—a review of methods. *Int J Mach Tools Manuf* 40:1073–1098
7. Jemielniak K (1999) Commercial tool condition monitoring systems. *Int J Adv Manuf Technol* 15:711–721
8. Choudhury IA, Baradie MA (1998) Machinability of nickel-based super alloys: a general review. *J Mat Proc Technol* 77:278–284
9. Jemielniak K (2006) Tool wear monitoring based on a non-monotonic signal feature. *Proc IMechE J Eng Manuf* 220(B2):163–170